Volcanic Unrest at Hakone Volcano after the 2015 phreatic eruption — Reactivation of a Ruptured Hydrothermal System?

Kazutaka Mannen (mannen@onken.odawara.kanagawa.jp)
Hot Springs Research Institute of Kanagawa Prefecture https://orcid.org/0000-0003-2816-0965
Yuki Abe
Hot Springs Research Institute of Kanagawa Prefecture
Yasushi Daita
Kanagawa Environmental Research Center
Ryosuke Doke
Hot Springs Research Institute of Kanagawa Prefecture
Masatake Harada
Hot Springs Research Institute of Kanagawa Prefecture
George Kikugawa
Hot Springs Research Institute of Kanagawa Prefecture
Naoki Honma
Japan Meteorological Agency
Yuji Miyashita
Hot Springs Research Institute of Kanagawa Prefecture
Yohei Yukutake
Hot Springs Research Institute of Kanagawa Prefecture

Full paper

Keywords: Hakone volcano, phreatic eruption, hydrothermal system, sealing zone, cap rock, volcanic unrest, scrubbing of magmatic gas

Posted Date: October 7th, 2020

DOI: https://doi.org/10.21203/rs.3.rs-86165/v1

Version of Record: A version of this preprint was published on March 26th, 2021. See the published version at https://doi.org/10.1186/s40623-021-01387-3.

Abstract

Since the beginning of the 21st century, volcanic unrest has occurred every 2–5 years at Hakone volcano. After the 2015 eruption, unrest activity changed significantly in terms of seismicity and geochemistry. In this paper, characteristics of the post-eruptive volcanic unrest that occurred in 2017 and 2019 are described, and changes in the hydrothermal system of the volcano caused by the eruption are discussed. Like the pre- and co-eruptive unrest, each post-eruptive unrest episode was detected by deep inflation below the volcano (~ 10 km) and deep low frequency events, which can be interpreted as reflecting supply of magma or magmatic fluid from depth. The seismic activity during the post-eruptive unrest episodes also increased; however, seismic activity beneath the eruption center during the unrest episodes was significantly lower, especially in the shallow region (~2 km), while sporadic seismic swarms were observed beneath the caldera rim, ~3 km away from the center. The 2015 eruption established routes for steam from the hydrothermal system (≥ 150 m deep) to the surface through the cap-rock, allowing emission of super-heated steam (~ 160 ºC), which was absent before the eruption. This steam showed an increase in magmatic/hydrothermal gas ratios (SO_2/H_2S and HCl/H_2S) in the 2019 unrest, which may be interpreted as magmatic intrusion at shallow depth; however, no indicative seismic and geodetic signals were observed. Net SO_2 emission during the post-eruptive unrest episodes, which remained within the usual range of the post-eruptive period, is also inconsistent with shallow intrusion. We consider that the post-eruptive unrest episodes were also triggered by newly derived magma or magmatic fluid from depth; however, the breached cap-rock was unable to allow subsequent pressurization of the hydrothermal system beneath the volcano center and suppressed seismic activity significantly. The heat released from the newly derived magma or fluid dried the vapor-dominated portion of the hydrothermal system and inhibited scrubbing of SO_2 and HCl to allow a higher magmatic/hydrothermal gas ratio. The 2015 eruption could have also breached the sealing zone near the brittle–plastic transition and the subsequent self-sealing process seems not to have completed based on the observations during the post-eruptive unrest episodes.

Introduction

Phreatic eruptions are eruption that have no direct involvement of magma and are instead driven by thermal energy of hydrothermal water. However, thermal energy itself is mainly provided by heat from magma, and recent geophysical observations revealed that deep intrusion of magma or magmatic fluid precedes phreatic eruptions. The time lag between such an intrusion and the eruption makes forecasting phreatic eruptions extremely challenging (Stix and De Moor 2018), as demonstrated by a series of eruptions of Ontake volcano in this decade.

The 2007 phreatic eruption of Ontake volcano was preceded by a magma intrusion approximately 3 km deep beneath the eruption center, which occurred approximately 2 months before the eruption (Nakamichi et al. 2009). In contrast, the 2014 phreatic eruption of the volcano, which killed more than 60 trekkers in the summit area, was only preceded by a volcano tectonic earthquake swarm that started 17 days before the eruption and no magmatic intrusion seems to have preceded it (Takagi and Onizawa 2016). However,

surprisingly, the ejecta of the 2014 eruption contained a trace amount of juvenile (magmatic material newly emplaced beneath the surface) fragments, and a series of geological investigations implied that the magmatic body intruded to 3 km deep beneath the volcano just before the 2007 eruption was released by the 2014 eruption (Miyagi et al. 2020). This sequence of eruptions implies that an eruption can be triggered by an intrusion event years prior. We thus cannot estimate eruption probability only based on intensity of volcanic unrest or source depth of deformation especially when a series of eruptions and/or unrest episodes have occurred at the volcano recently. For such a volcano, evaluation of volcanic unrest based on the model of a magma-hydrothermal system is critical to avoid underestimation of eruption probability.

Hakone volcano, located near the nation's capital Tokyo, is one of the largest tourist destinations in Japan and attracts more than three million tourists annually to the center of phreatic eruption named Owakudani (Owakidani) steaming area (Fig. 1). In this volcano, volcanic unrest episodes have repeated every few years since the beginning of the 21st century, and eventually in 2015, a small phreatic eruption occurred at Owakudani steaming area (Mannen et al. 2018). Even after this eruption, volcanic unrest continued to take place, and evaluation of these events has yet to be done. Here we summarize the recent volcanic unrest and discussion the possibility of future phreatic eruptions.

Background

Hakone Volcano and its activity in the 21st century

Here we review Hakone volcano and its latest activity based on Mannen et al. (2018). Hakone is a caldera volcano located at approximately 80 km SW of Tokyo (Fig. 1a). Its eruption history started at least 400 ka and after two caldera-forming stages. Andesitic effusive eruptions since 40 ka have formed a complex of lava flows and domes named the Younger Central Cones (YCC) in the center of the caldera (Fig. 1b). The latest magmatic eruption occurred near the northernmost part of YCC and formed a lava dome named Kanmurigatake, which erupted within an amphitheater that was created by a sector collapse just before the dome formation. The most active steaming area and the center of the latest phreatic eruptions named Owakudani is located at the eastern flank of Kanmurigatake.

Hakone is not very active in terms of magmatic eruptions; however, it is notable for its high seismicity, with at least 7 intensive earthquake swarms observed in the 20th century. Most of the swarms did not accompany clear intensification of steaming activity, while the volcanic unrest from 1933 to 1935 culminated with a formation of a new steam vent 1 km south of Owakudani, although the exact location of the vent is not known.

The continuous instrumental monitoring of Hakone volcano started after the volcanic unrest of 1959–60; however, the volcano monitoring network detected no major seismic swarm until 2001. The 2001 unrest accompanied an earthquake swarm, and deep and shallow inflation as observed by Global Navigation Satellite System (GNSS) and a tiltmeter network, and culminated with a blowout of a steam production

well (SPW) in Owakudani (500 m deep). Since the 2001 unrest, major volcanic unrest episodes comprising earthquake swarms, deep inflation detected by a GNSS network, and deep low frequency events (DLF) were observed in 2006, 2008–2009 and 2013 (Harada et al. 2018; Yukutake et al. 2019). In terms of seismicity, these events can be intensive as historical unrest episodes before 1960. These volcanic unrest episodes were not accompanied by significant increases of steaming activity in the steaming areas of the volcano; however, in March 2015, a new volcanic unrest episode started with a deep inflation and increase of both volcano-tectonic and DLF seismicity. This volcanic unrest was followed by a blowout of SPW in early May, and eventually, on June 29, a small phreatic eruption started and lasted until the early morning of July 1. The 2015 volcanic unrest after the eruption seems to have continued until late August, which is evident from crustal inflation monitoring by GNSS (Harada et al. 2018).

Subsurface structure of Hakone volcano

Various geophysical and geochemical investigations over the last decade have modeled the subsurface structure of Hakone volcano. They are summarized in Fig. 2 and as follows. At approximately 20 km beneath the northern caldera rim of the volcano, DLFs occur sporadically. Since many of the DLF swarm events were followed by inflation of the edifice and shallow volcano-tectonic earthquake swarms, DLFs are interpreted as a signal indicating migration of magmatic fluid (Yukutake et al. 2015, 2019). A seismic tomography study revealed velocity structure beneath Hakone volcano and showed that the volcano has an active magma-hydrothermal system (Yukutake et al. 2015). Yukutake et al. (2015) identified a high-Vp/Vs and low Vs body (Region 1), which was considered to represent a magma chamber located at approximately 10 km depth. Above Region 1, a low-Vp/Vs and low-Vs body (Region 2) was identified and interpreted as a fluid-rich zone. The upper boundary of the Region 2 is shallower than 5 km, and interestingly, the boundary seems to reach near the surface just beneath Owakudani. Above Region 2 is the fracture zone, where most of the volcano tectonic earthquakes occur. Some fraction of the earthquakes in the fracture zone of Hakone volcano can be attributed to re-activation of pre-existing fractures caused by fluid migrations (Yukutake et al. 2010, 2011). Significant anisotropy in the shallow crust beneath Hakone volcano also indicates pre-existing fractures that are controlled by the regional stress field (Honda et al. 2014). The fracture zone and Region 2 overlap slightly and both are considered to form the hydrothermal system.

A magnetotelluric study in and around Hakone volcano revealed a bell-shaped conductive body beneath the volcano, the top of which reaches the surface near Owakudani (Yoshimura et al. 2018). Since the bell-shaped conductive body nests a resistive body beneath it, they are considered represent the hydrothermal system of the volcano. The bell-shaped body is interpreted as a smectite-rich zone, which was formed by a prolonged hydrothermal activity of the volcano. In Owakudani and the surrounding area (Fig. 1), a series of local high-resolution magnetotelluric surveys was conducted and revealed that the bell-shaped conductive body is exposed on the surface in the bottom of Owakudani valley (Mannen et al. 2019). A geological investigation of a borehole showed that the bell-shaped conductive body corresponds to altered volcanic sediment accompanying smectite as predicted by Yoshimura et al. (2018) (Mannen et al.

2019). Epicenters of volcano tectonic earthquakes at Hakone are located within the resistive body (i.e. hydrothermal system) (Yoshimura et al., 2018). Peculiarly, seismic signals other than volcano tectonic earthquakes, such as shallow volcanic tremor and low frequency events, are rare in this volcano. The shallow non volcano-tectonic earthquakes detected by our network are a single isolated very shallow M = − 0.3 event that occurred near Owakudani during the 2006 unrest (Tanada et al. 2007) and tremors sourced from the boiling conduit during the 2015 eruption (Yukutake et al. 2017). Since shallow tremors and low frequency earthquakes are common in volcanoes that have active hydrothermal systems, the paucity of shallow seismic signals related migration of fluids even during volcanic unrest episodes could be a significant feature of Hakone volcano.

Geochemical monitoring has provided evidence for development of a sealing zone and injection of magmatic fluid into the hydrothermal system through the zone (Ohba et al. 2019). Very shallow geological and resistivity structures (≤ 500 m deep) are summarized in Mannen et al. (2019); the very shallow inflation source of the 2015 eruption (Doke et al. 2018; Kobayashi et al. 2018), which was interpreted as a vapor pocket located 150 m deep beneath the eruption center (surface elevation is approximately 1000 m above sea level) was determined by a high-resolution magnetotelluric survey (CSAMT) as a high resistivity zone within the apex of the bell-shaped conductive body (Yoshimura et al. 2018).

The 2015 eruption and unrest

The time sequence of the 2015 unrest and eruption of Hakone volcano was already summarized in Mannen et al. (2018). Here we briefly review this event. The onset of the 2015 unrest was first recognized in early April from increases in DLFs and the baseline length across the volcano detected by GNSS, which were interpreted as inflation of magma chamber due to addition of magma or magmatic fluid (Harada et al. 2018; Mannen et al. 2018; Yukutake et al. 2019) (Fig. 3). Then an earthquake swarm, a blowout of SPW, and an increase in the CO_2/H_2O ratio of the fumarole gas emitted near the future eruption center followed (Mannen et al. 2018; Ohba et al. 2019). Although the seismicity and the CO_2/H_2O ratio began decreasing after mid-May, a small phreatic eruption occurred on the morning of June 29 and lasted until the early morning of July 1 (Yukutake et al. 2017; Mannen et al. 2018). The eruption was seemingly triggered by formation of an open crack in the morning of June 29 near the surface (830–854 m above sea level) to deeper than 530 m above sea level as indicated by satellite InSAR and analysis of records obtained by broadband seismometers and tilt meters (Doke et al. 2018; Honda et al. 2018). However, chemical and component analyses of the erupted ash and water indicated a shallow (shallower than 850 m above sea level or 150 m deep from the surface) origin (Mannen et al. 2019). Even after the eruption, shallow and deep inflation (0.8 km and − 6.5 km above sea level, respectively) continued without a significant change in the inflation rate until August (Harada et al. 2018). The seismicity began in the central part of the caldera and then propagated to the peripheral areas (Fig. 4a)

The 2017 unrest episode

The 2017 unrest of Hakone volcano was subtle to detect based on seismicity. Seismicity rates in 2017 were generally low and only 242 earthquakes were detected in the Hakone area by the routine analysis of Hot Springs Research Institute. This annual number is within the range of that in an ordinary year without volcanic unrest after 2000 (Fig. 5). However, slight increases of seismicity were observed in mid-April and early May at sea level beneath Mt. Kintoki at the northern rim of the caldera (Fig. 4b). Concurrently, in early May, the baseline length crossing Hakone volcano began to increase slowly and continued to increase until early November (Fig. 3). Daita et al. (2020) reported an increase in the CO_2/H_2S (C/S) ratio of fumarole gas in Kamiyu, a steaming area north of Owakudani. The increases in C/S ratio have been observed accompanying the volcanic unrest; however, this increase in C/S ratio was not sharp and did not attenuate swiftly, unlike the increases in C/S ratio accompanying the 2013 and 2015 unrest episodes (Daita et al. 2019; Ohba et al. 2019) (Fig. 3). An increase in DLF events was also observed in early April (Fig. 3).

The 2019 unrest episode

The 2019 unrest episode at Hakone volcano appears to have begun with a slight increase in seismicity in March, which lasted until the end of October. A sudden seismic swarm occurred on May 18 beneath the western caldera rim (Fig. 4c). Although the location of swarm events was remote from Owakudani (3 km west and outside of the latest eruption centers), the number of earthquakes exceeded a set criterion and the Japan Meteorological Agency (JMA), which is in charge of volcano monitoring and alerting, announced a rise in Volcano Alert Level (VAL) from 1 to 2 for the volcano in the early morning of May 19, and the VAL2 continued until October 7. The baseline length crossing Hakone volcano began to increase in mid-March and continued until the beginning of August. The C/S ratio of Kamiyu also began to increase after the end of April; however, the increase in C/S ratio was not sharp and again did not attenuate quickly, similar to the 2017 unrest episode (Fig. 3). During the volcanic unrest, ratios of magmatic gases such as SO_2 and HCl relative to H_2S, which is a hydrothermal gas, increased significantly in Owakudani, although a significant net increase in magmatic gas was not observed by a Differential Optical Absorption Spectroscopy (DOAS) campaign (Fig. 7) (Abe et al. 2018). A slight increase in DLF events at the beginning was also observed during the unrest; however, interestingly, a far larger number of DLFs was observed in the latest phase of the unrest in late October (Fig. 3).

Data

Field surveys after the eruption

Since the entry of researchers around the eruption center was allowed after the 2015 eruption (beginning in March 2016), we have monitored fumarole temperature and chemical compositions of volcanic gases and hot spring waters. Here we summarize these results.

Fumarole temperature

New fumaroles, which emit superheated steam (> 100 ºC) were created in the eruption center area in 2015. Most of them were formed during the eruption but some formed during the unrest phase before the eruption or even long after the eruption. Until the present, steam temperatures have been routinely measured for at least 20 fumaroles, five of which are relatively intensive and long-lived and are shown in Fig. 6 (see Fig. 1c for the locations). The maximum temperature among them (164.3 ºC) were recorded on April 10, 2018 at the 15 − 1 fumarole, which is the fumarole created in the main crater formed during the eruption (Mannen et al. 2019). As shown in Fig. 6, steam temperatures are not decreasing for all fumaroles. However, a decline of the maximum temperature in the steaming area is detected, at a rate of ~ 7.7 ºC/yr, using infrared images of the whole area taken continuous since early 2016 (Harada 2018). These observations imply a waning trend in thermal activity in the eruption center area as a whole, while several stable fumaroles constantly emit superheated steam from depth (probably ~ 150 m deep; Mannen et al. 2019). It is noteworthy that no temperature change related to the volcanic unrest in 2017 and 2019 was apparant from these observations.

SO_2 emission from Owakudani steaming area

We conducted DOAS surveys to quantify emission rates of SO_2 from the Owakudani steaming area (Abe et al. 2018; Fig. 7). SO_2 emission from Owakudani reached more than 100 t/day just after the 2015 eruption; however, the emission rate decreased rapidly and is now estimated to be approximately 10 t/day. The DOAS measurements contain large errors (up to 2–8 t/day) and no significant increase in SO_2 during volcanic unrest episodes in 2017 and 2019 was measured.

Fumarole gas

An accurate chemical analysis of volcanic gas requires meticulous sampling and complicated lab procedures (Ozawa 1968), limiting the monitoring frequency. We thus launched a long-term test of simple gas measurements using a detector tube named Passive Dosi-tube (GASTEC Co. Ltd. (GASTEC 2018)). For this study, two sets of dositubes composed of H_2S, SO_2 and HCl sensors (GASTEC No. 5D, 4D and 14D respectively) were installed near (2–4 m) the 15 − 2 fumarole vent (Fig. 1c). A set of dositubes is directly exposed to the air while another set is installed in a 500 ml ventilated container filled with silica-gel granules (150 g) to prevent condensation of water in and around the dositubes. The dositubes were expected to measure ratios of volcanic gas in the atmosphere near the fumarole rather than a direct measurement of steam emitting from the volcano; thus, the observed ratio may be altered by processes in the atmosphere such as gas absorption by water droplets in the steam. However, we aimed to monitor obvious sequential changes in gas ratios with high frequency measurements. Since the dositube measures the volume fraction of the target gas in the atmosphere, the gas ratio is volumetric ratio (i.e., molar ratio) assuming an ideal gas. The sequential change of SO_2/H_2S and HCl/H_2S ratios, both of which indicate the ratio of magmatic gas to hydrothermal gas, are shown in Fig. 8. Since the start of monitoring (March in 2018), SO_2/H_2S ratio show a constant decrease, and HCl remained nearly undetected until March 2019. However, both SO_2/H_2S and HCl/H_2S ratios started to increase after March

2019 and peaked around June 2019. Since then, both SO_2/H_2S and HCl/H_2S ratios showed a gradual decline; however, both ratios are still higher than those before March 2019 at the time of writing (mid 2020).

Soil gas

Near the Owakudani steaming area, volcanic gas is seeping out from the soil under a building floor (Loc. 3 in Fig. 1c). We made weekly measurements of CO_2 and H_2S in the ventilated air from under the building floor using detector tubes since the end the eruption (Fig. 9). Since the volcanic gas emitted from soil is not affected by nearby rainfall, and the building ventilation system enables almost constant flux of air from the subfloor, we can expect stable measurements of emitted gas. The soil gas shows a constant increasing in H_2S while CO_2 remains almost stable. Interestingly, both H_2S and CO_2 show subtle increases during the 2017 and 2019 unrest episodes. The CO_2/H_2S ratio (hereafter C/S ratio) decreased almost constantly after the 2015 eruption; however, slight increases can be recognized during the 2017 and 2019 unrest episodes.

Artificial hot springs

In Owakudani, artificial hot springs (AHS) have been created by mixing steam from SPW and spring water pumped up from the caldera floor to supply the local hotel industry (Mannen et al. 2019). AHS is not a diluted condensation of steam from the production well because less-soluble gases such as CO_2 and H_2S are barely absorbed in the water; however, its chemistry can be useful to monitor the hydrothermal system beneath the steaming area. We routinely analyzed the chemistry of AHSs from SPWs, No. 52 and No. 39 (hereafter SPW52 and SPW39 respectively; see Fig. 1c for locations). Here we show temporal changes of Cl and SO_4 content, which are possibly magmatic in origin, and major anions in the AHSs (Fig. 10).

SPW52, which is 500 m deep and the well that blew out during the 2001 unrest, had shown a continuous decrease in Cl of the AHS since the beginning of monitoring; however, after early April just before the onset of the 2017 unrest, Cl content spiked. The Cl content again a showed constant decrease after the end of the 2017 unrest; however, it increased significantly when the baseline length across Hakone volcano started to increase (early May in 2019). The Cl content of SPW39 (413 m deep) also showed an unrest-related increase. For both AHSs, contrary to Cl, SO_4 shows no significant change even during the volcanic unrest episodes.

River water from the eruption center

The eruption center area forms the headstream of the Owakuzawa river. Thus, water from Owakuzawa is presumably affected by volcanic gas and natural hot springs within the area, and its chemical components can reflect hydrothermal activity. Indeed, just after the 2015 eruption, water from the river showed a significant increase in Cl and SO_4 (Fig. 10; Mannen et al. 2018). After the eruption, the Cl and

SO_4 contents showed constant decline; however, they apparently rose slightly at the beginning of the 2019 unrest. The Cl and SO_4 changes related to the 2017 unrest were ambiguous (Fig. 10).

Seismicity related to volcanic unrest after the 2015 eruption

We examined the depth variation of seismic events within the hydrothermal system to detect any changes related to the eruption. Figure 11 shows the cumulative ratio of earthquakes within the hydrothermal system beneath Owakudani during volcanic unrest episodes in this century. Interestingly, the seismicity depth change from before and after the eruption seems to be significant. Before the 2015 eruption, epicenters of more than 60% of earthquakes in and around the Owakudani steaming area were located shallower than 2 km depth, while such earthquakes comprise less than 40% of the total after the eruption. This observation indicates that the fraction of shallower earthquakes declined significantly after the 2015 eruption.

Discussion

Lowered VT activity and depressurization of the hydrothermal system

The 2015 eruption and post-eruptive unrest episodes appear to have been triggered by inflation at depth (Kobayashi et al.2018; Mannen et al. 2018) (Fig. 12a and b). Similar deep inflation was also recognized since the earliest phase of the post-eruptive unrest episodes in 2017 and 2019 by GNSS monitoring. DLFs were also detected in the earliest phase of the pre-, co-, and post-eruptive unrest. However, subsequent seismicity seems to be different for the post-eruptive unrest episodes. VT earthquakes beneath the central cone were not as prevalent during the post-eruptive unrest episodes, especially in the shallow region (Fig. 11), although significant seismic activity took place beneath the caldera rim, remote from the active fumarole (A and B in Fig. 4). Assuming pore-pressure increase is the trigger for VT seismicity (Yukutake et al. 2011; Mannen et al. 2018), such a significant difference can be interpreted as lower pore pressure rise in the hydrothermal system beneath the central cone, especially in the shallower part of the hydrothermal system (< 4 km deep). The insufficient pressurization of the hydrothermal system comparing to the pre-eruptive unrest episodes can be explained by the destruction of the cap-rock of the volcano by the 2015 eruption (Fig. 12c and d).

Mannen et al (2019) concluded that the materials erupted in the 2015 eruption was derived from cap-rock based on geological and magnetotelluric analyses. The enthalpy of the maximum temperature of steam emitted from the fumarole (2805 kJ/kg, 164.3 ºC at the surface) is very close to that of saturated steam coexisting with liquid water at ~ 200 ºC and ~ 1.5 MPa, which is a hydrothermal condition at the depth of 150 m assuming hydrostatic pressure. Magnetotelluric surveys and InSAR analysis indicate that a vapor-rich portion of the hydrothermal system is located approximately 150 m below the surface of the eruption center and named the portion ‘vapor pocket’ (Doke et al. 2018; Kobayashi et al. 2018; Mannen et al. 2019). This line of evidence implies that the 2015 eruption tapped vapor from the uppermost part of the

hydrothermal system and some vapor routes through the cap-rock created by the eruption are still alive as indicated by surviving high temperature fumaroles (≥ 160 ºC). Such degassing routes after the eruption can inhibit pressurization of the hydrothermal system during an unrest episode. The higher resistivity of the enlarged vapor pocket after the eruption (Mannen et al. 2019) indicates an increase in the vapor phase, presumably due to depressurization caused by the breach of the cap-rock (Fig. 12c). The intensive seismic and hydrothermal activities during the 2015 activity may have increased the permeability of the hydrothermal system beneath Owakudani and contributed to the inhibition of pressure increase in the region during the post-eruptive unrest (Sibson et al. 1975).

Even though the eruption breached the cap-rock beneath Owakudani, pore pressure seems to have increased in other hydrothermal systems in the adjacent area during the post-eruptive unrest episodes. The seismic swarm beneath the northern (2017; A in Fig. 4b) and western (2019; B in Fig. 4c) caldera rim during the unrest episodes could be the manifestion of fluid injection from depth to the separated hydrothermal systems that caused a pore pressure rise and fluid migration as observed in the previous unrest (Yukutake et al. 2011), although a detailed analysis remains yet to be done (Fig. 12d).

Increase of magmatic gas during the post-eruptive unrest

During the post-eruptive unrest episodes, magmatic gas species, such as SO_2, HCl and CO_2 were observed to increase compared to H_2S, which is a representative hydrothermal gas. In particular, since HCl tends to be degassed from shallow magma (Rouwet et al. 2017), this suggest intrusion and degassing of shallow magma during the post-eruptive unrest. However, no indication of shallow intrusion, such as low frequency earthquakes and harmonic tremor, was observed in our geophysical monitoring. Also, our DOAS survey observed no significant gross increase in SO_2 emissions. The emissions of SO_2 during the post-eruptive unrest episodes were less than the standard criterion to indicate magma involvement (> 100 t/d) (Symonds et al. 2001).

SO_2 and HCl are magmatic, but they are highly soluble in liquid water. We thus attribute the increase of these gases to a change in liquid-vapor ratio in the uppermost part of the hydrothermal system (~ 150 m deep). In the environment where liquid water exists, SO_2 and HCl can be scrubbed from the coexisting volcanic gas; thus the increase of these gases can imply drying-out of the hydrothermal system (Symonds et al. 2001). Since the fumarole temperatures showed no significant increase during the post-eruptive unrest episodes (Fig. 6), significant heating of the hydrothermal system that vaporized liquid water in the shallowest hydrothermal system is highly improbable. Instead, a slight increase of heat-flux changed the liquid–vapor ratio in the uppermost part of the hydrothermal system (~ 150 m deep) without any change of temperature in the system. The increase of heat-flux may be attributed to the injection of hot and pressurized magmatic fluid into the hydrothermal system by the rupture of the sealing zone at depth, possibly at the brittle-ductile transition (Fig. 12c and d).

Previous model of volcanic unrest

Ohba et al. (2019) proposed another unrest mechanism for Hakone volcano, which is possible even without newly derived magmatic fluid from depth but instead steady degassing of magma. They emphasized the increase of atmospheric gases such as Ar and N_2 in the fumarole emissions a few months before the onset of the 2015 unrest and interpreted this as the development of a sealing zone between the hydrothermal and magma-peripheral systems. During the pre-unrest phase, permeability of the sealing zone decreased and the pressure of magmatic gas represented by CO_2 beneath the sealing zone increased. Meanwhile, pressure in the hydrothermal system dropped due to the lack of influx of magmatic gas from the magma-peripheral system, allowing atmospheric gas to seep into the hydrothermal system, as detected by their survey of the fumarole gas.

This is an interesting model that interprets the results of gas monitoring; however, the model neglects geophysical observations such as deep inflation and DLFs in the early phase of the volcanic unrest episodes. If the deep inflation was caused by pressurization of volatile species beneath the sealing zone, deflation should have occurred after the breach of the sealing zone. Also, the DLF events in the very early phase of the unrest episodes indicates injection of magma or magmatic fluid from depth. We acknowledge that it is hard to explain the increase of atmospheric species in the fumarole during the pre-unrest phase; however, we point out that this was observed only in fumarole N, which is located near the eruption center of the 2015 eruption. This means that the injection of atmospheric species seems to have occurred only in a very limited part of the hydrothermal system, probably near the surface of the steaming area. In the steaming area, reactivation of an almost extinct steam production well (SPW39) was recognized on April 17 (Mannen et al. 2018) and inflation of the steaming area was recognized by InSAR on May 7 (Doke et al. 2018). These observations indicate that underground fracturing and a local uplift ($\leq$ 200 m in diameter) due to very shallow inflation could have started before May 2015. Indeed, fracturing of the surface was visually observed after mid-June (Mannen et al. 2018) and such fracturing may have introduced air into the shallowest region of the hydrothermal system near the uplift region. The small hydrothermal system that underwent contamination by atmospheric gas species may be the vapor pocket located approximately 150 m deep beneath the center of the 2015 eruption (Mannen et al. 2018).

Degassing of CO_2 during the unrest episodes and its implication

The increase in C/S ratio from the very early phase of the unrest episodes at Hakone volcano can be explained by a breach of the sealing zone that leads to a significant pressure contrast between the hydrothermal system and a CO_2 reservoir beneath it. The sealing zone may not be necessarily be identical to the brittle-ductile transition as implied by Ohba et al. (2018). However, it is noteworthy that no significant change in SO_2 and H_2S emission had been recognized in the peripheral fumaroles around the eruption center (Ohba et al., 2018). This means that only CO_2 was injected into the hydrothermal system, implying magma degassing deeper than the levels of SO_2 and H_2S exsolution but shallower than that of CO_2. The breach of the sealing zone and the migration of the hydrothermal fluid from the magma-

peripheral to the hydrothermal systems might have accompanied bubbling of CO_2 (Lowenstern 2001), although no corresponding geophysical signal was observed.

Degassing from newly-derived magmatic fluid may have been the source of the CO_2 and the reason for the increase in the C/S ratio; however, the 2017 and the 2019 unrest episodes did not show sharp increases in the C/S ratio even though these events were accompanied by DLFs. Such a difference in the temporal change in C/S ratio during the volcanic unrest episodes indicates a change in physical structure caused by the 2015 eruption. We previously proposed a breach of the shallow cap-rock in. In addition to that, we propose a breach of the deep sealing zone during the 2015 eruption, with its annealing process after the eruption still incomplete. Assuming the sealing zone remained breached, volatiles steadily degassed from the magma chamber cannot be stored beneath the sealing zone in large quantity (Fig. 12c). Thus, only newly derived magmatic fluid may contribute to the CO_2 rise during the volcanic unrest, and the observed CO_2 increase at the surface became subtle as observed during the unrest episodes in 2017 and 2019 (Fig. 12d). Based on this model, we expect that the sequential change of C/S ratio characterized by a strong increase just after the beginning of an unrest and a strong decrease after the climax as observed in 2013 and 2015 (Fig. 3) will resume after a restoration of the sealing zone in the future.

Model caveats

Deep inflation sources during Hakone unrest episodes have been located using inversion analysis; however their optimum depths were not unique; ranging from 6.5 km for the 2015 unrest and eruption (Harada et al. 2018) to 10 km for the 2019 unrest (Doke et al. 2019). Mannen et al. (2018) interpreted deep inflation during Hakone unrest episodes indicated by GNSS analysis as magma replenishment. Kobayashi et al. (2018) located the source of the deep inflation during the 2015 unrest and eruption (4.8 km deep) and considered the inflation source to represent a magma chamber. However, these source depths are shallower than Region 1, which is considered as representing a magma chamber from seismic tomography, and rather located in the hydrothermal system (Yukutake et al. 2015). We may thus need to assume magma intrusion or accumulation of magmatic fluid in the deeper part of the hydrothermal system. As discussed above, intrusion of magma to the hydrothermal system is possible but relatively low emission of magmatic gases observed may contradict the model. Accumulation of magmatic fluid within the deeper part of the hydrothermal system may be indicating a larger phreatic eruption in future as post eruptive deflations were observed after major eruptions occurred in Ontake in 2014 (Murase et al. 2016; Narita and Murakami 2018) and Te Maari in 2012 (Hamling et al. 2016) but not after the 2015 eruption of Hakone volcano. Since intrusion of magmatic fluid at depth can occur without significant seismic and geodetic precursors as shown by the 2014 eruption of Ontake (Takagi and Onizawa 2016), we should be alert even to minor volcanic unrest episodes.

Conclusion

The volcanic unrest episodes of Hakone volcano observed after its latest phreatic eruption in 2015 were reviewed. Like the pre- and co-eruptive unrest, the post-eruptive unrest episodes that occurred in 2017 and 2019 were accompanied by inflation of the volcano and deep low frequency events, both of which can be interpreted as a magma replenishment to the deep magma chamber (~ 10 km). Seismicity during the post-eruptive unrest episodes was, however, significantly lower than that of pre- and co-eruptive unrest episodes of the volcano, especially in the shallower portion of the hydrothermal system. Such minimal seismicity can result from a breach of the cap-rock during the 2015 eruption, which inhibited pore pressure accumulation within the hydrothermal system beneath it. Accompanying the post eruptive unrest episodes, increases of magmatic components such as SO_2, HCl and CO_2 relative to a hydrothermal component H_2S of fumarole gas were observed. Amounts of Cl^- in an artificial hot spring generated by steam from deep steam production wells and river water were found to have increased. Intrusion of magma to shallow depth is, however, improbable given the stable fumarole temperature, the lack of non-tectonic earthquakes (low frequency event and harmonic tremor), and limited SO_2 emission (< 100 t/d). Instead, the increased proportion of magmatic gas (SO_2 and HCl) relative to the hydrothermal gas (H_2S) during the 2019 unrest implies depletion of the liquid phase in the shallowest portion of the hydrothermal system due to the increased heat flux from depth.

The sealing zone of the volcano, presumably located near the brittle-ductile boundary, also seems to have been breached by the 2015 eruption as no sharp rise in the C/S ratio of the fumarole gas was observed during the post-eruptive unrest episodes. The sharp rise of the C/S ratio can be interpreted as a release of CO_2 that had accumulated beneath the sealing zone. We thus anticipate re-establishment of the temporal C/S change as seen during the pre-eruptive unrest episodes after the complete re-establishment of the sealing zone. The rupture of cap-rock by the 2015 eruption may lower the possibility of future phreatic eruptions originating from the shallow hydrothermal system; however, accumulation of magmatic fluid in the deeper part of the hydrothermal system cannot be ruled out, and the possibility of a future large phreatic eruption cannot be eliminated.

Abbreviations

CSAMT, Controlled Source Audio-frequency Magneto Telluric

InSAR, Interferometric synthetic-aperture radar

JMA, Japan Meteorological Agency

SPW, steam production well for making hot spring water in Owakudani.

Declarations

Ethics approval and consent to participate

Not applicable

Consent for publication

Not applicable

Availability of data and materials

The datasets, that was used to created figures in this paper appears in Supplementary Information before the publication.

Competing interests

The authors declare that they have no competing interests

Funding

This study was implemented as an ordinary research project of HSRI.

Authors' contributions

KM engaged in geological observation and drafted the manuscript compiling multidisciplinary data. YD has routinely measured C/S ratio of volcanic gas. YA and MH conducted DOAS surveys. MH and RD analyzed GNSS data. GK, YM and NH implemented sampling and chemical analysis of waters. YY analyzed DLF. All authors reviewed and approved the final manuscript.

Acknowledgements

Hakone Town Office and Hakone Onsen Kyokyu Co. Ltd helped with our field survey. Takeshi Ohba at Tokai University kindly offered his volcanic gas data. Hakone Geomuseum kindly provided their gas data of the Loc. 3. This manuscript was greatly improved by helpful English editing by Diana Roman (Carnegie Institution for Science).

Authors' information

Not applicable

Endnotes

Not applicable

References

1. Abe Y, Harada M, Itadera K, Mori T, Takagi A (2018) Emission rate of sulfur dioxide at Owakudani, Hakone volcano, Japan – Observation, analysis, and temporal transition of emission rate to June 2018 –. Bull Hot Springs Res Inst Kanagawa Prefect 50:1–18

2. Daita Y, Ohba T, Yaguchi M, Sogo T, Harada M (2019) Temporal variation of the fumarolic gas composition (C/S ratio) in 2017 at north side slope of Owakudani geothermal area, Hakone volcano. Bull Hot Springs Res Inst Kanagawa Prefect 51:37–44
3. Doke R, Harada M, Itadera K, Kato T (2019) Crustal deformation associated with the 2019 earthquake swarm activity of Hakone volcano observed by GNSS. Bull Hot Springs Res Inst Kanagawa Prefect 51:1–9
4. Doke R, Harada M, Mannen K, Itadera K, Takenaka J (2018) InSAR analysis for detecting the route of hydrothermal fluid to the surface during the 2015 phreatic eruption of Hakone Volcano, Japan. Earth, Planets Sp. doi: 10.1186/s40623-018-0834-4
5. GASTEC (2018) Gastec Handbook: Environmental analysis technology 18th edition
6. Hamling IJ, Williams CA, Hreinsdõttir S (2016) Depressurization of a hydrothermal system following the August and November 2012 Te Maari eruptions of Tongariro, New Zealand. Geophys Res Lett 43:168–175. doi:10.1002/2015GL067264
7. Harada M (2018) Characteristics of continuous observation by infrared thermal camera at Owakudani, Hakone volcano. Bull Hot Springs Res Inst Kanagawa Prefect 50:53–59
8. Harada M, Doke R, Mannen K, Itadera K, Satomura M (2018) Temporal changes in inflation sources during the 2015 unrest and eruption of Hakone volcano, Japan. Earth Planets Sp 70:152. doi:10.1186/s40623-018-0923-4
9. Honda R, Yukutake Y, Morita Y, Sakai S, Itadera K, Kokubo K (2018) Precursory tilt changes associated with a phreatic eruption of the Hakone volcano and the corresponding source model. Earth Planets Sp. doi:10.1186/s40623-018-0887-4
10. Honda R, Yukutake Y, Yoshida A, Harada M, Miyaoka K, Satomura M (2014) Stress-induced spatiotemporal variations in anisotropic structures beneath Hakone volcano, Japan, detected by S wave splitting: A tool for volcanic activity monitoring. J Geophys Res Solid Earth 119:7043–7057. doi:10.1002/2014JB011151.Received
11. Kobayashi T, Morishita Y, Munekane H (2018) First detection of precursory ground inflation of a small phreatic eruption by InSAR. Earth Planet Sci Lett 491:244–254. doi:10.1016/j.epsl.2018.03.041
12. Lowenstern JB (2001) Carbon dioxide in magmas and implications for hydrothermal systems. Miner Depos 36:490–502. doi:10.1007/s001260100185
13. Mannen K, Tanada T, Jomori A, Akatsuka T, Kikugawa G, Fukazawa Y, Yamashita H, Fujimoto K (2019) Source constraints for the 2015 phreatic eruption of Hakone Volcano, Japan, based on geological analysis and resistivity structure. Earth Planets Sp 71:135. doi:10.1186/s40623-019-1116-5
14. Mannen K, Yukutake Y, Kikugawa G, Harada M, Itadera K, Takenaka J (2018) Chronology of the 2015 eruption of Hakone volcano, Japan – geological background, mechanism of volcanic unrest and disaster mitigation measures during the crisis. Earth Planets Sp 70:68. doi:10.1186/s40623-018-0844-2

15. Miyagi I, Geshi N, Hamasaki S, Oikawa T, Tomiya A (2020) Heat source of the 2014 phreatic eruption of Mount Ontake, Japan. Bull Volcanol 82:33. doi:10.1007/s00445-020-1358-x
16. Murase M, Kimata F, Yamanaka Y, Horikawa S, Matsuhiro K, Matsushima T, Mori H, Ohkura T, Yoshikawa S, Miyajima R, Inoue H, Mishima T, Sonoda T, Uchida K, Yamamoto K, Nakamichi H (2016) Preparatory process preceding the 2014 eruption of Mount Ontake volcano, Japan: insights from precise leveling measurements. Earth Planets Sp 68:9. doi:10.1186/s40623-016-0386-4
17. Nakamichi H, Kumagai H, Nakano M, Okubo M, Kimata F, Ito Y, Obara K (2009) Source mechanism of a very-long-period event at Mt Ontake, central Japan: Response of a hydrothermal system to magma intrusion beneath the summit. J Volcanol Geotherm Res 187:167–177. doi:10.1016/j.jvolgeores.2009.09.006
18. Narita S, Murakami M (2018) Shallow hydrothermal reservoir inferred from post-eruptive deflation at Ontake Volcano as revealed by PALSAR-2 InSAR. Earth Planets Sp 70:191. doi:10.1186/s40623-018-0966-6
19. Ohba T, Yaguchi M, Nishino K, Numanami N, Daita Y, Sukigara C, Ito M, Tsnogai U (2019) Time variations in the chemical and isotopic composition of fumarolic gases at Hakone volcano, Honshu Island, Japan, over the earthquake swarm and eruption in 2015, interpreted by magma sealing model. Earth Planets Sp 71:48. doi:10.1186/s40623-019-1027-5
20. Ozawa T (1968) Chemical analysis of volcanic gases: I. Chemical analysis of volcanic gases containing water vapor, hydrogen chloride, sulfur dioxide, hydrogen sulfide, carbon dioxide, etc. Geochemistry Int 5:939–947
21. Rouwet D, Hidalgo S, Joseph EP, González-Ilama G (2017) Fluid Geochemistry and Volcanic Unrest: Dissolving the Haze in Time and Space. pp 221–239
22. Sibson RH, Moore JMM, Rankin AH (1975) Seismic pumping—a hydrothermal fluid transport mechanism. J Geol Soc London 131:653–659. doi:10.1144/gsjgs.131.6.0653
23. Stix J, De Moor MJ (2018) Understanding and forecasting phreatic eruptions driven by magmatic degassing. Earth, Planets Sp. doi: 10.1186/s40623-018-0855-z
24. Symonds RB, Gerlach TM, Reed MH (2001) Magmatic gas scrubbing: Implications for volcano monitoring. J Volcanol Geotherm Res 108:303–341. doi:10.1016/S0377-0273(00)00292-4
25. Takagi A, Onizawa S (2016) Shallow pressure sources associated with the 2007 and 2014 phreatic eruptions of Mt. Ontake Japan Earth Planets Sp 68:135. doi:10.1186/s40623-016-0515-0
26. Tanada T, Honda R, Harada M, Yukutake Y, Ito H (2007) Earthquake activity in Kanagawa Prefecture and its adjacent area in 2006. Catfish Lett Hot Springs Res Inst Kanagawa Prefect 57:1–12
27. Yoshimura R, Ogawa Y, Yukutake Y, Kanda W, Komori S, Hase H, Goto T, Honda R, Harada M, Yamazaki T, Kamo M, Kawasaki S, Higa T, Suzuki T, Yasuda Y, Tani M, Usui Y (2018) Resistivity characterisation of Hakone volcano, Central Japan, by three-dimensional magnetotelluric inversion. Earth Planets Sp 70:66. doi:10.1186/s40623-018-0848-y
28. Yukutake Y, Abe Y, Doke R (2019) Deep Low-Frequency Earthquakes Beneath the Hakone Volcano, Central Japan, and their Relation to Volcanic Activity. Geophys Res Lett 1–9.

doi:10.1029/2019GL084357

29. Yukutake Y, Honda R, Harada M, Arai R, Matsubara M (2015) A magma-hydrothermal system beneath Hakone volcano, central Japan, revealed by highly resolved velocity structures. J Geophys Res Solid Earth 120:3293–3308. doi:10.1002/2014JB011856.Received
30. Yukutake Y, Honda R, Harada M, Doke R, Saito T, Ueno T, Sakai S, Morita Y (2017) Continuous volcanic tremor during the 2015 phreatic eruption in Hakone volcano. Earth, Planets Sp. doi: 10.1186/s40623-017-0751-y
31. Yukutake Y, Ito H, Honda R, Harada M, Tanada T, Yoshida A (2011) Fluid-induced swarm earthquake sequence revealed by precisely determined hypocenters and focal mechanisms in the 2009 activity at Hakone volcano, Japan. J Geophys Res Solid Earth 116:1–13. doi:10.1029/2010JB008036
32. Yukutake Y, Tanada T, Honda R, Masatake H, Ito H, Yoshida A,ß (2010) Fine fracture structures in the geothermal region of Hakone volcano, revealed by well-resolved earthquake hypocenters and focal mechanisms. Tectonophysics 489:104–118

Figures

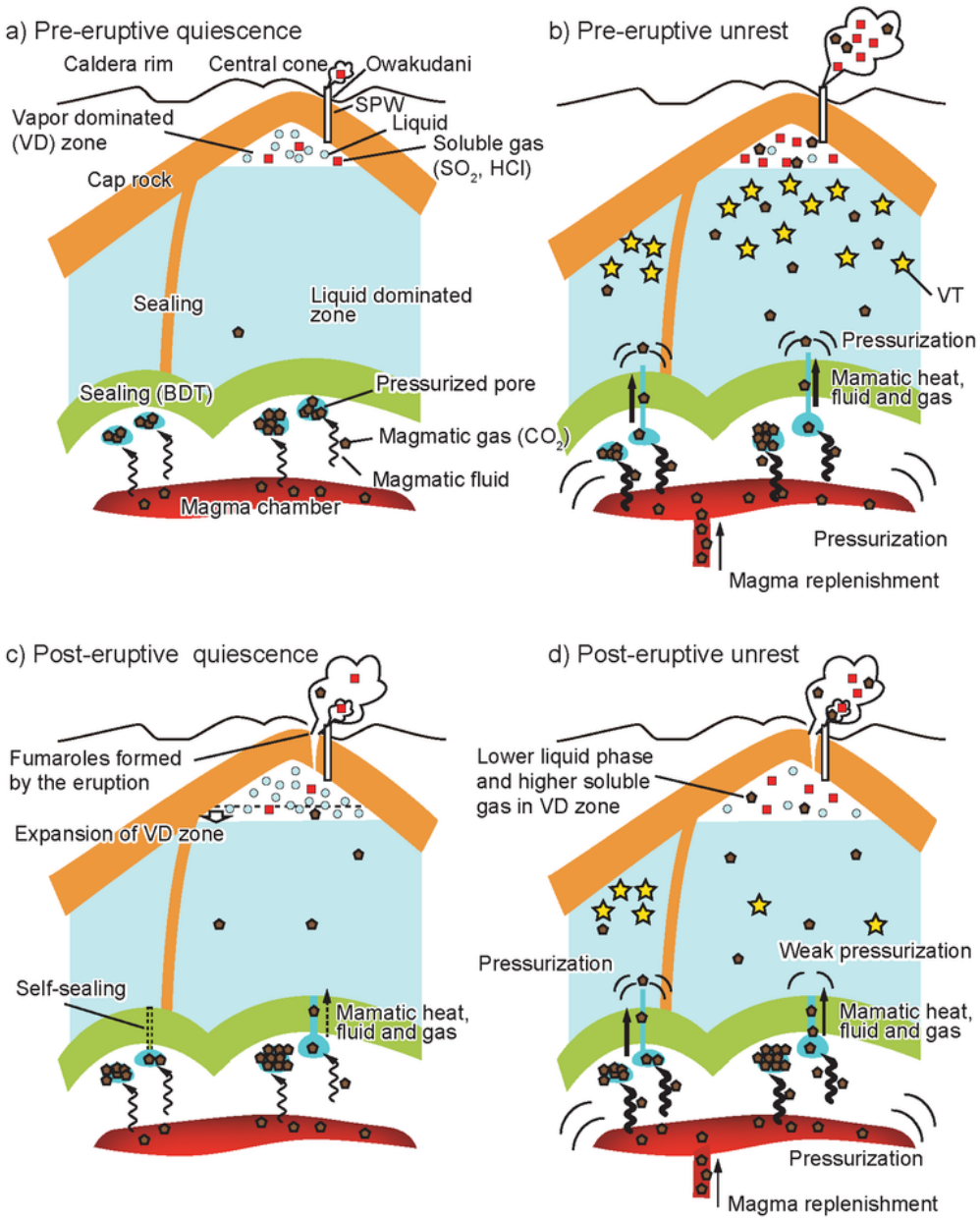

Figure 1

Index map of Hakone volcano. a) Location of Hakone volcano. b) Topographical map of Hakone volcano. c) Sampling locations. Blue lines indicate the Owakuzawa River and its tributary. Red star, soil gas location; yellow circle, fumarole; green square, steam production well (SPW). The two digits before the hyphen indicate year of emergence (e.g. 15-2 was formed in 2015).

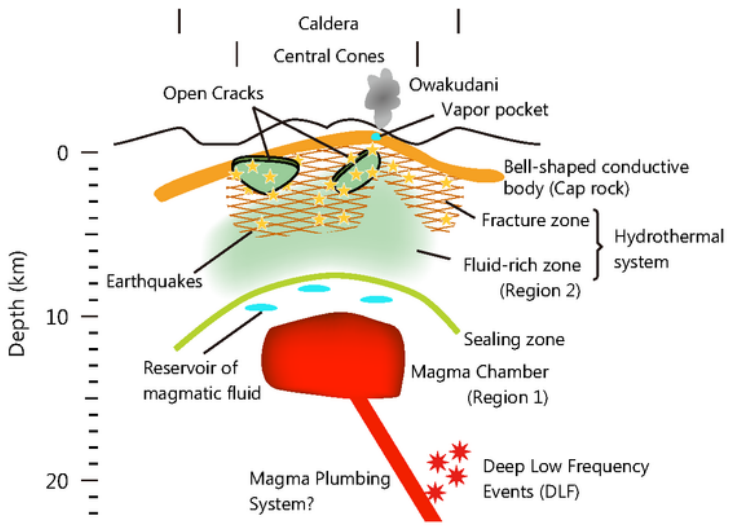

Figure 2

A schematic model of subsurface structure of Hakone volcano. This model is modified version of a previous model (Yukutake et al. 2015; Mannen et al. 2018) based on recent studies (Doke et al. 2018; Kobayashi et al. 2018; Yoshimura et al. 2018; Mannen et al. 2019; Ohba et al. 2019; Yukutake et al. 2019).

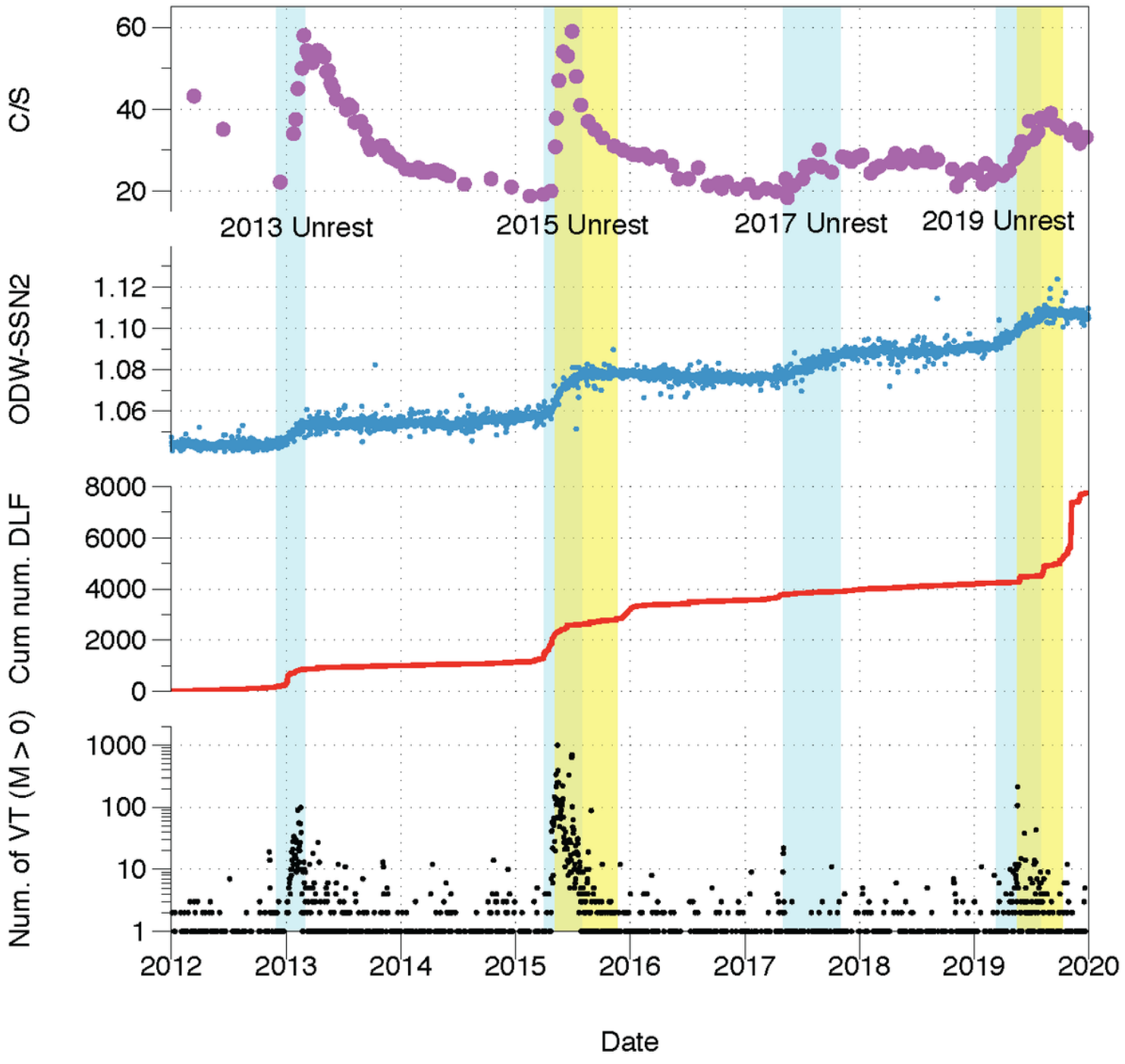

Figure 3

Sequential change of a) CO2/H2S (C/S) molar ratio of fumarole gas emitted from Site S at Owakudani (after Daita et al., 2019; Ohba et al, 2018), b) baseline length across Hakone volcano (Odawara – Susono2 + 20747 m), c) cumulative number of deep low frequency events, and d) daily number of volcano tectonic earthquakes in Hakone volcano. Durations of VAL 2 or more are shown as yellow hatches (May 6 to Nov. 20 for 2015 and May 19 to Oct. 9 for 2019) and durations of volcanic unrest

defined as periods of baseline increase are shown as blue hatch (December 1, 2012 to March 1, 2013, April 1 to August 1 of 2015, May 1 to Nov 1 of 2017 and March 1 to August 1 of 2019).

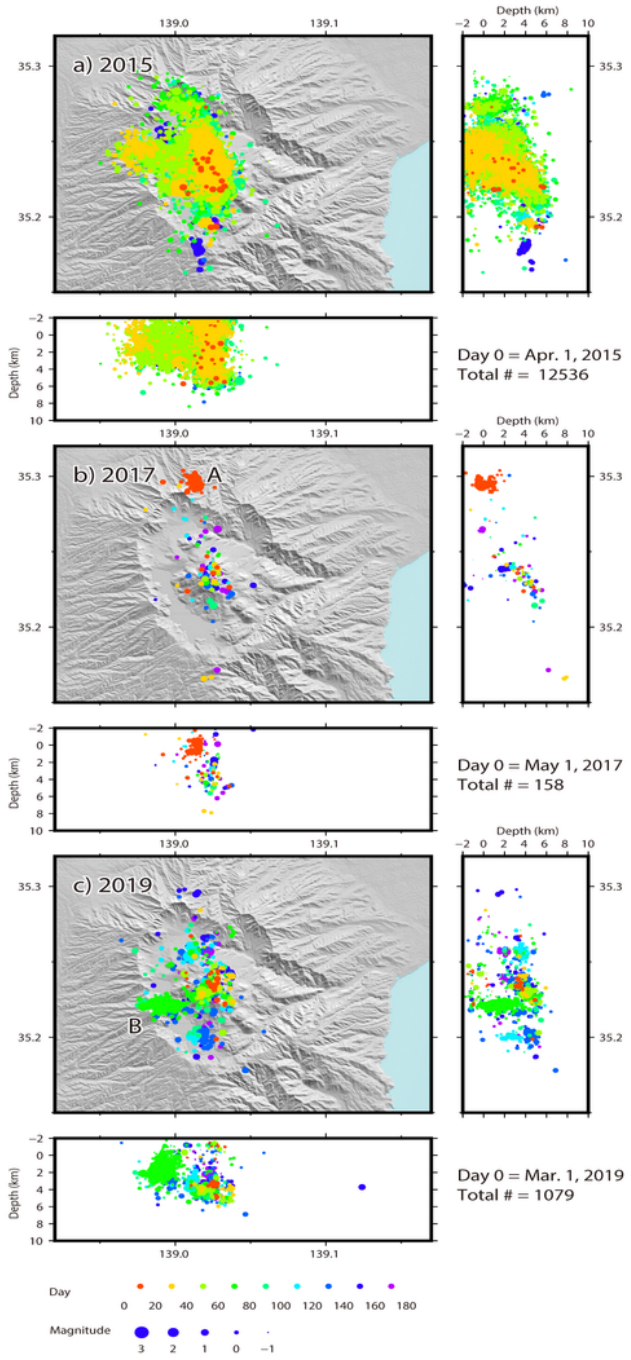

Figure 4

Maps of hypocenters of volcano-tectonic earthquakes during the co-eruptive (2015) and post-eruptive (2017 and 2019) volcanic unrest episodes. Day 0 is set to the first day of a month during which onset of the edifice inflation was observed and shown in the bottom-right corner of each panel. Hypocenters of

earthquakes that occurred within 180 days after day 0 are plotted. Colors indicate days after day 0 and the radius of each circle indicates magnitude of the earthquake. The total number of earthquakes during the 180 days are shown in the bottom-right corner of each panel. A in b) indicates the earthquake swarm in early May in 2017. B in c) indicates the swarms on 18 and 19 of May in 2019.

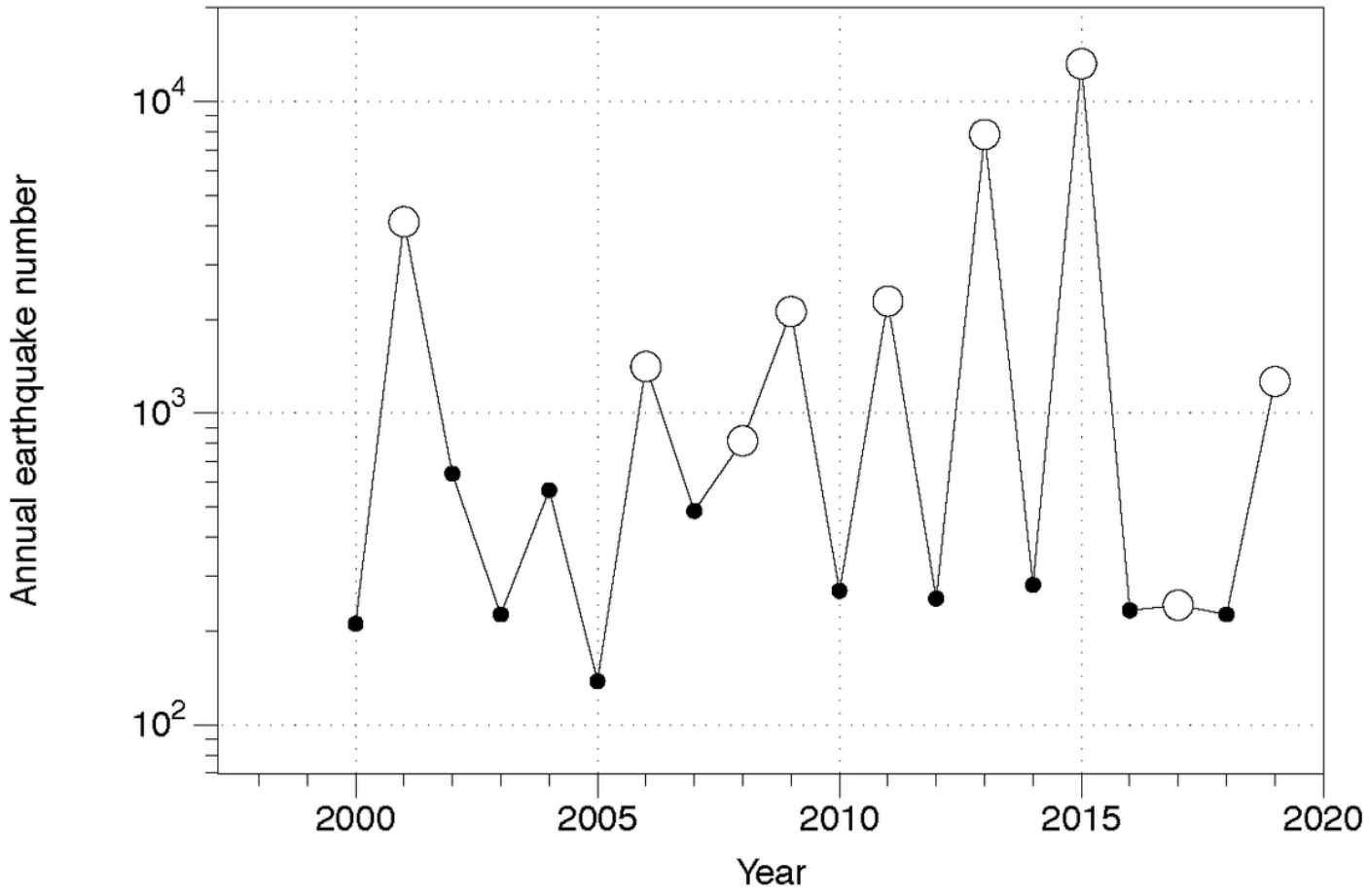

Figure 5

Annual number of volcano tectonic earthquakes in Hakone volcano detected by routine analysis of HSRI. Open circles indicate years that underwent volcanic unrest while dots indicate years without unrest.

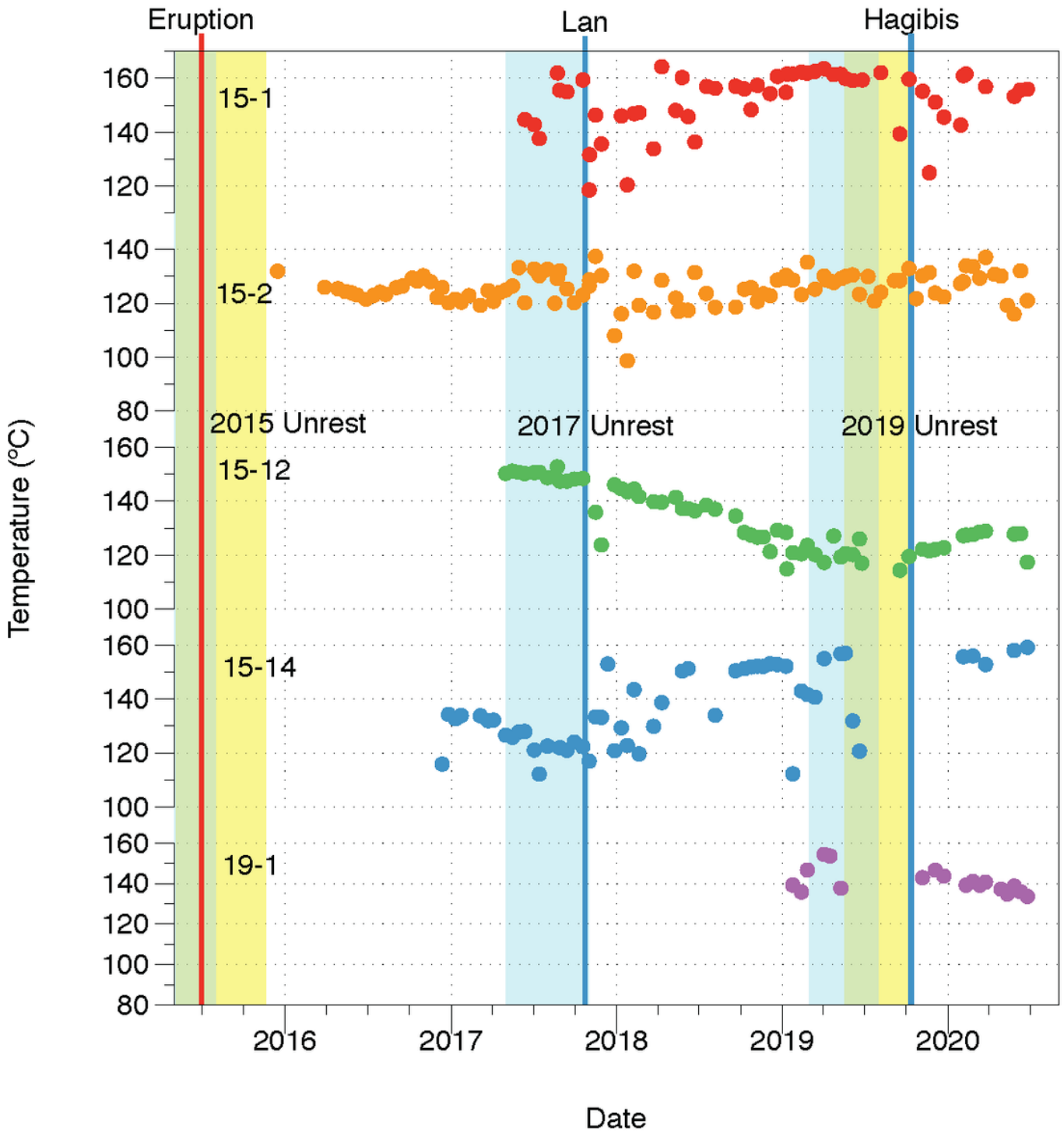

Figure 6

Temporal changes in temperature of steam emitted from fumaroles in Owakudani. The durations of volcanic unrest episodes are shown as shaded yellow (VAL2 or more) and blue (baseline across the volcano is increasing). See caption of Figure 3 for details. Timing of heavy rains due to typhoons, which seem to have temporarily lowered steam temperature from some fumaroles, is also shown (Lan on October 23 in 2017 and Hagibis on October 18, 2019). The location of fumaroles is shown in Figure 1c.

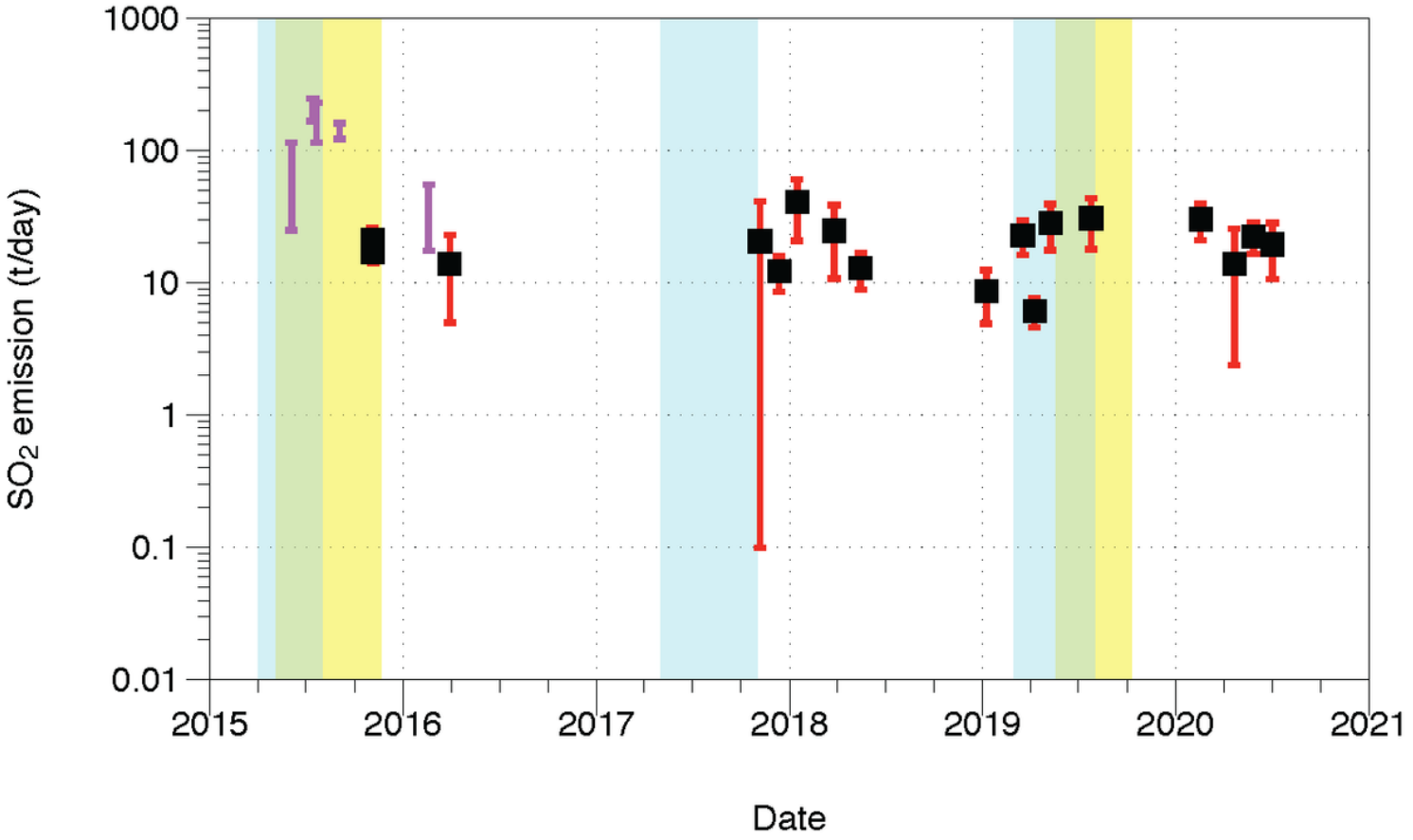

Figure 7

Sequential change of SO2 emission from Owakudani steaming area. Green circles with error bars indicate measurements by the Hot Springs Research Institute of Kanagawa Prefecture while others (error bars only) are measurements by JMA.

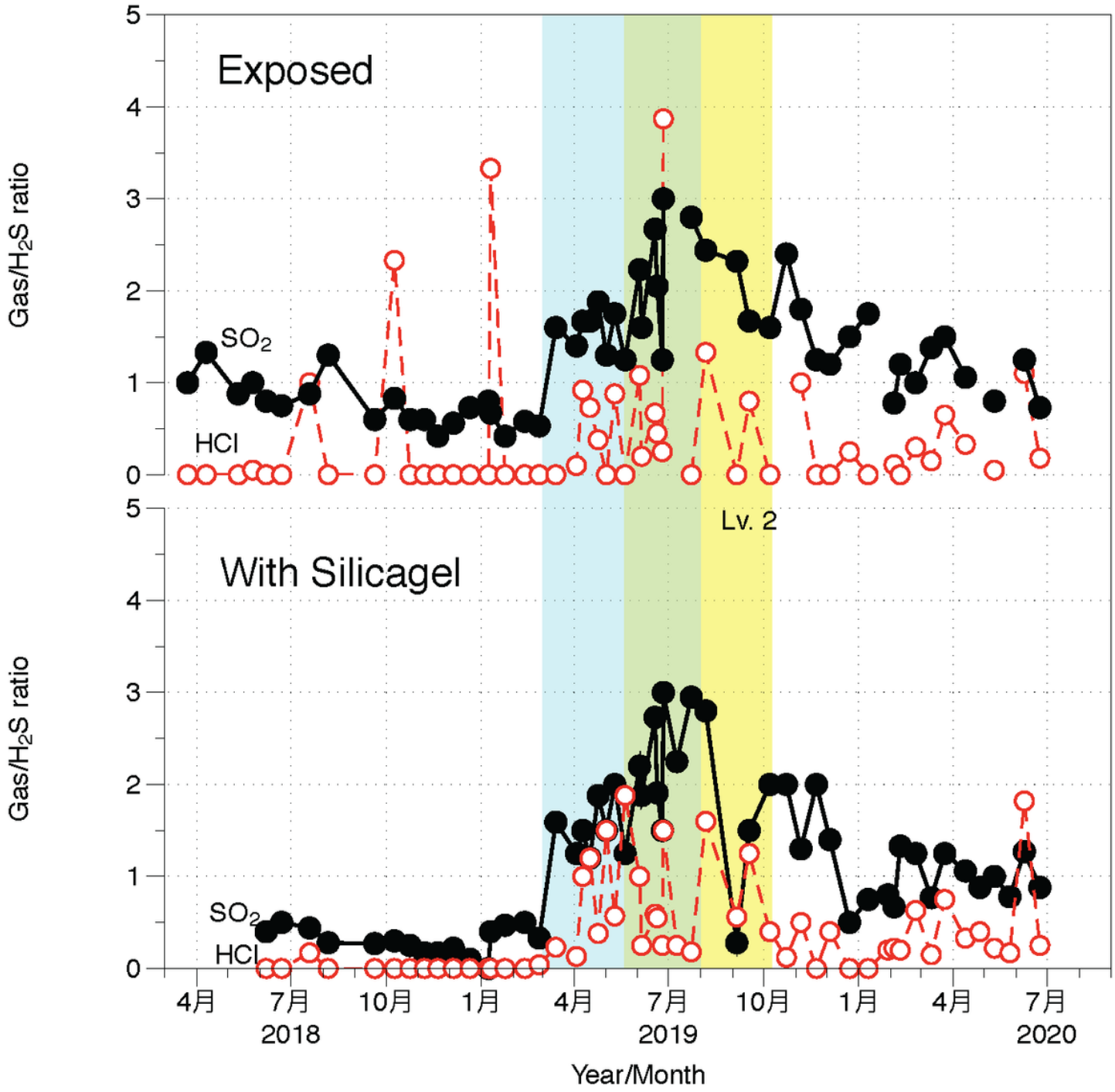

Figure 8

Sequential change of magmatic components (SO2 and HCl) relative to a hydrothermal component (H2S) within the atmosphere near the 15-2 fumarole, measured by dositubes. Each panel shows values obtained by a set of dositubes exposed to the air (upper panel) and another set within a container filled with silica-gel (lower panel). The durations of volcanic unrest episodes are shown as shaded yellow (VAL2 or more) and blue (baseline across the volcano is increasing). See caption of Figure 3 for details.

The spikes in HCl/H2S ratio of the exposed set (HCl/H2S > 2) are considered to be errors caused by color changes due to steam precipitation within the tube.

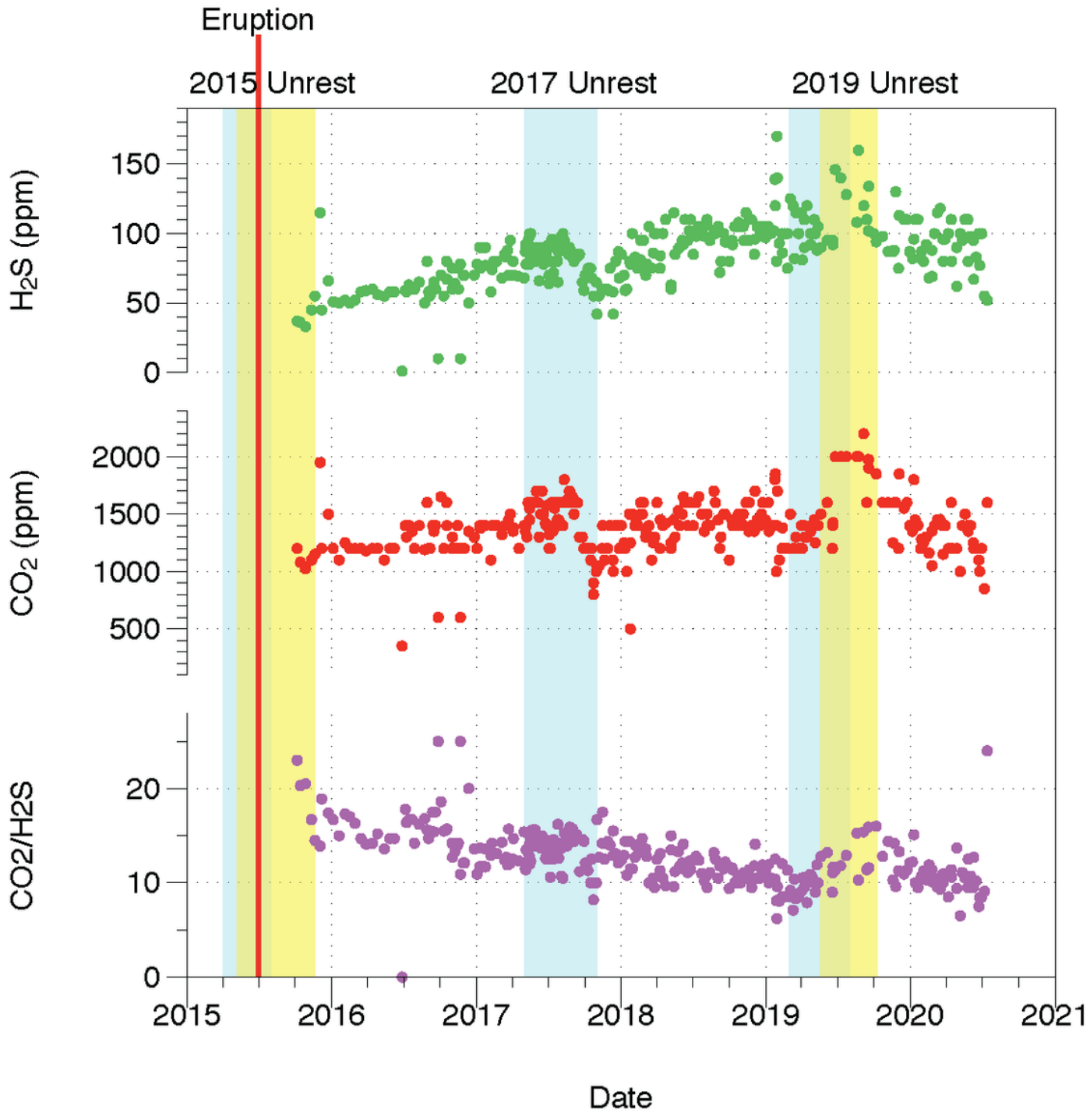

Figure 9

Sequential change in the volcanic component of soil gas near the center of the 2015 eruption (Loc. 3 in Figure 1c). The durations of volcanic unrest episodes are shown as shaded yellow (VAL2 or more) and blue (baseline across the volcano is increasing). See caption of Figure 3 for details.

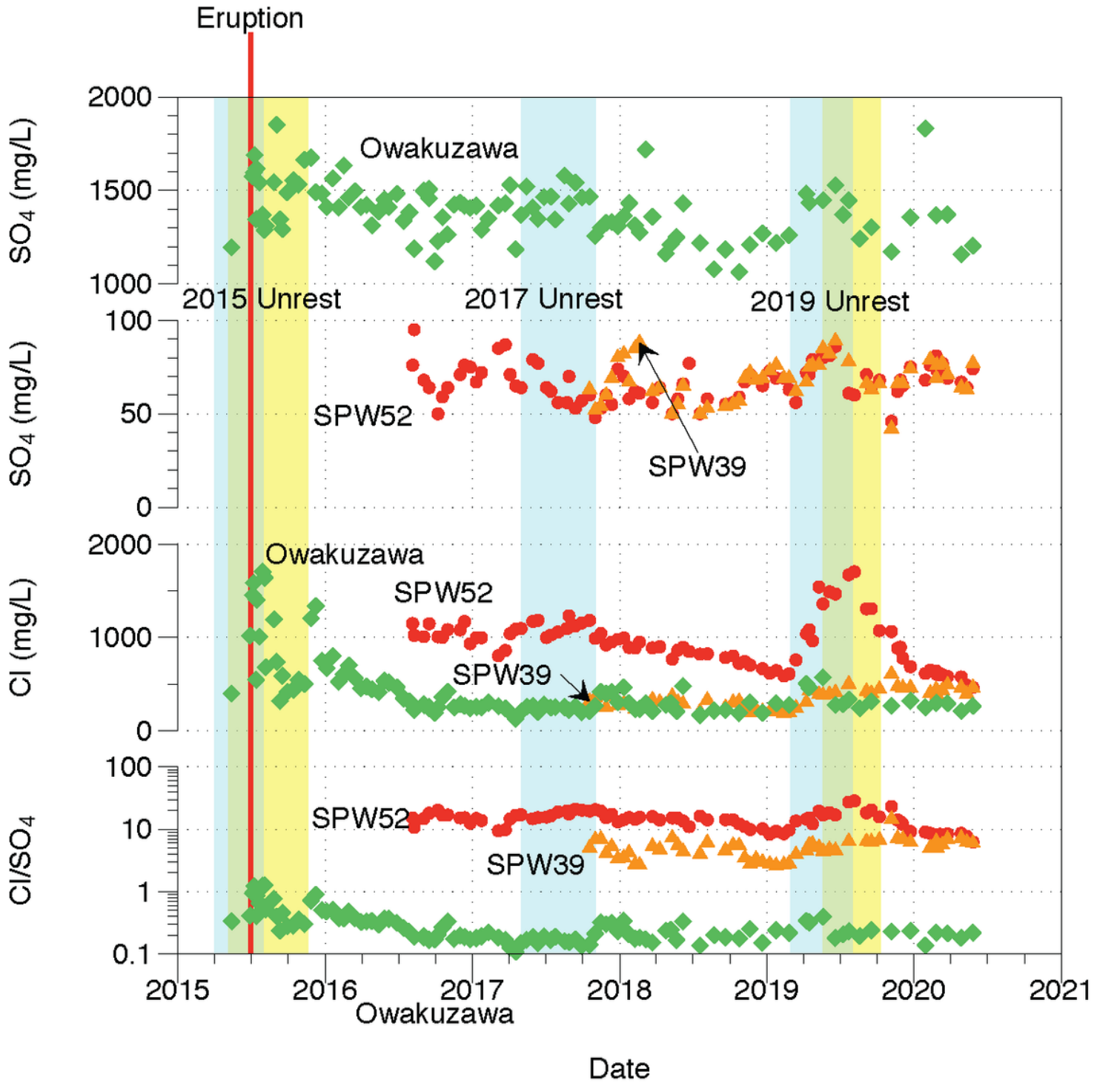

Figure 10

Sequential changes in the chemistry of artificial hot springs created by the steams from SPW52 (red circle) and SPW39 (orange triangle), and water from the Owakuzawa river (green diamond).

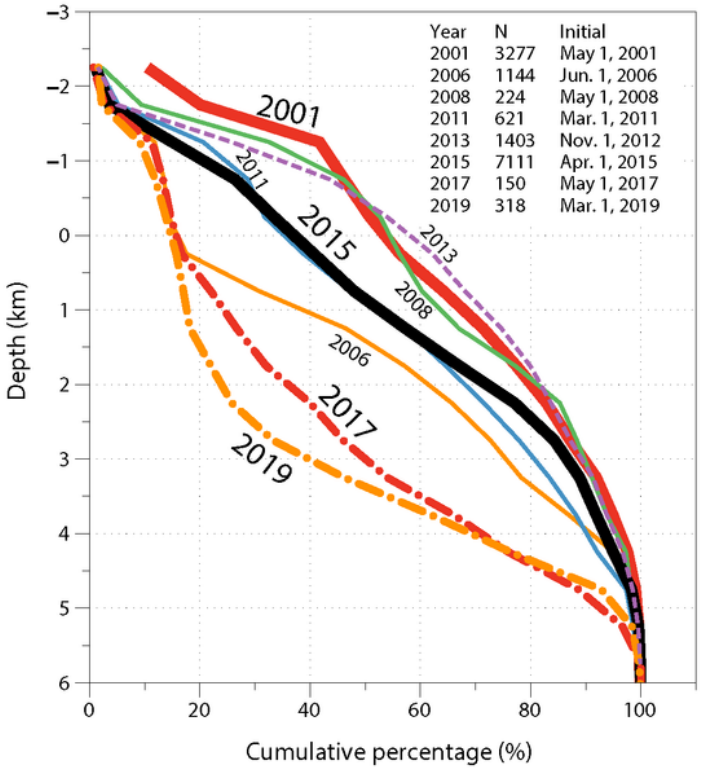

Figure 11

Frequency–depth variations of volcano tectonic earthquakes in the hydrothermal system during post-2001 volcanic unrest episodes We count the number of earthquakes with epicenters within 2 km of the summit of Kamiyama (35.2333º N 139.0208 º E). Here, the earthquakes during volcanic unrest are defined as those occurring within 6 months of the initial date. The initial dates and total number of

earthquakes (N) are shown in the upper right of the figure. Note that epicenter depths for earthquakes shallower than 0 km are not well-constrained.

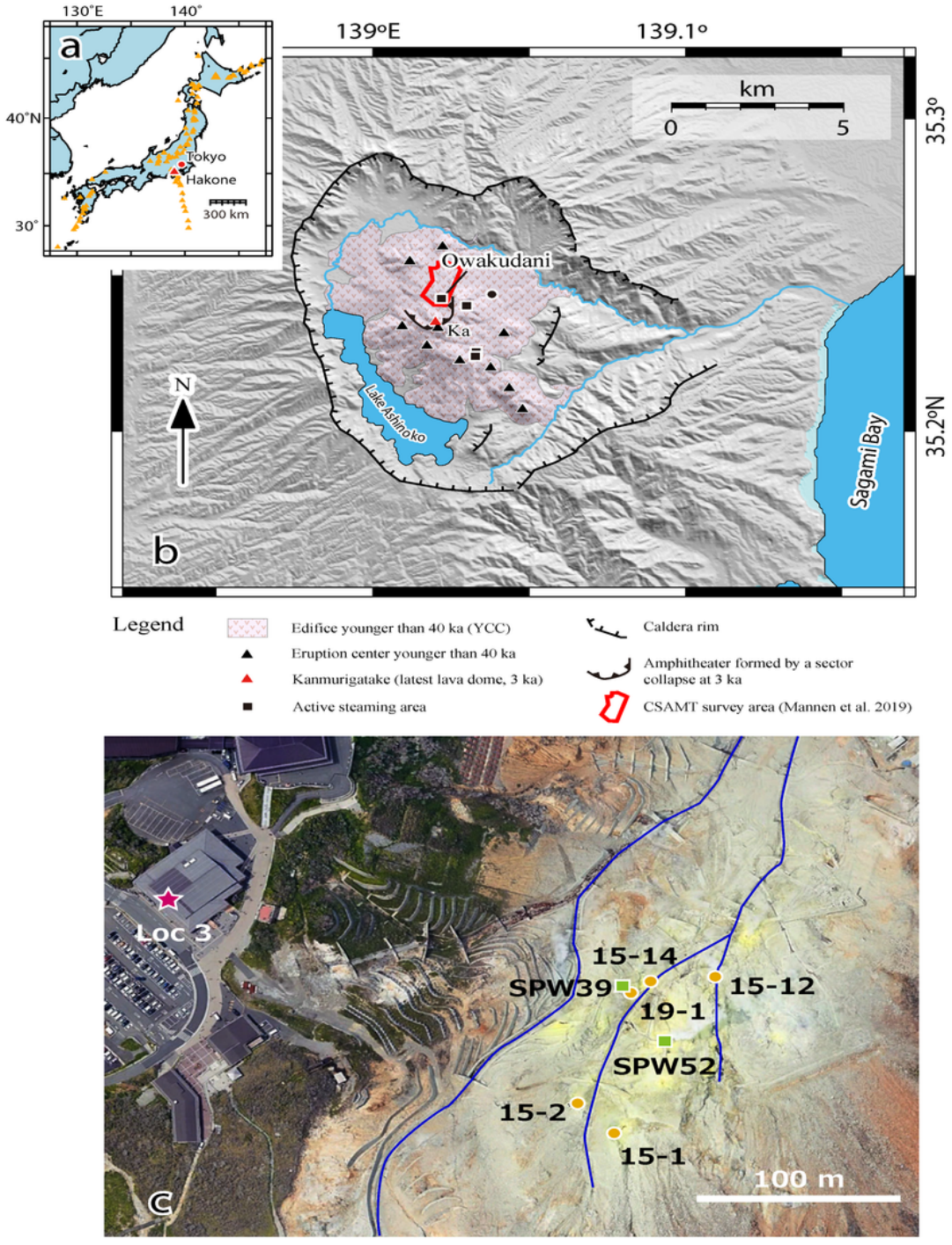

Figure 12

Schematic model of the pre- and post-eruptive hydrothermal systems. Not drawn to scale. See text for depth and dimension of the features. a) Before the 2015 eruption, cap-rock and sealing at the brittle-ductile transition (BDT) were intact and magmatic gas accumulated within the pressurized pores beneath

the BDT. We assume individual hydrothermal systems beneath the central cones and caldera rim are separated by a seal. b) Ruptures of sealing at the BDT induced by a magma replenishment event allowed rapid migration of accumulated heat, fluid and pore pressure beneath the BDT to the liquid-dominated zones of the hydrothermal systems. Volcano-tectonic earthquakes (VTs) and steaming from the steam production wells (SPW) increased due to the pressurization of the hydrothermal system. c) The 2015 eruption formed paths for steam from the vapor dominated (VD) zone to the surface. Due to the path, the post-eruptive hydrothermal system beneath the central cone was depressurized and volume of the VD zone increased. The rupture of seals at the BDT healed beneath the caldera rim, but were maintained beneath the central cones, which allows migration of heat and pore fluid beneath the BDT. d) Post-eruptive unrest episodes were also triggered by magma replenishment. Beneath the central cones, no extensive pressurization of the hydrothermal system occurs because pores beneath the BDT were not pressurized due to the rupturing in the 2015 eruption. Heat migration from deep to shallow lowered the liquid phase fraction within the VD zone and caused less effective scrubbing, which allowed enrichment of soluble gas (SO_2 and HCl) within the steams from the VD zone and fumaroles. Magmatic CO_2 within the fumaroles also rose; however, not significantly due to the absence of release of accumulated CO_2 within the pressurized pores beneath the BDT.

Supplementary Files

This is a list of supplementary files associated with this preprint. Click to download.

- Fig00graphicabstract.pdf